Materials Science in Semiconductor Processing 89 (2019) 105–109

Contents lists available at ScienceDirect

Materials Science in Semiconductor Processing

journal homepage: www.elsevier.com/locate/mssp

Electron field emission from graphene nanosheets grown on Si nanoporous pillar array

Zhaojun Tang[a,b], Sen Li[a], Zheng Zhu[a], Xinjian Li[a,*]

[a] Department of Physics and Laboratory of Material Physics, Zhengzhou University, Zhengzhou 450052, People's Republic of China
[b] Electrical Engineering Department, Zhengzhou Business Technician Institute, Zhengzhou 450100, People's Republic of China

ARTICLE INFO

Keywords:
Graphene nanosheet
Si nanoporous pillar array
Field emission
Flat lying

ABSTRACT

Graphene nanosheet (GNS) thin film was grown flat lying on Si nanoporous pillar array (Si-NPA) substrate using Ni nanocrystallites as catalyst by a chemical vapor deposition method, and its field electron emission characteristics were studied. The thin film was proved to be composed of high-quality few-layer GNSs with a typical size of ~6 nm. With a turn-on field of ~2.85 V/μm, an emission current density of ~53.9 μA/cm^2 was obtained at an electric field of 4.2 V/μm. Based on the experimental data, the enhancement factor of few-layer GNS/Si-NPA was calculated to be ~2700 according to the Fowler–Nordheim theory. The cold cathode also showed higher emission stability than vertically standing graphene at low operating voltages. For comparison, GNS/Si-NPA with multi-layer GNSs was prepared and its turn-on field was obtained as high as 8.5 V/μm. The origin of the high emission performance was attributed to numerous emission sites formed at the edges of GNSs, unique structure and morphology of GNS/Si-NPA, and low electric resistance of GNSs. Our results might have provided an alternative approach for fabricating Si-based low-voltage cold cathodes with high device performances.

1. Introduction

Among the field emission (FE) cathode materials developed in the past decades, various carbon materials, such as carbon nanotubes (CNTs) [1–4], carbon nanofibers [5], diamond or diamond-like films [6–8] and fullerenes [9,10], have been expected highly as potential candidates for cold cathodes due to low electron affinity and chemical and mechanical stability. In particular, carbon nanotube (CNT) becomes a recent focus of attention because it possesses stable electron emission with low turn-on fields and big forward emission current densities (ECD) [11]. However, the extensive application of CNT-based cathodes is seriously baffled by some inherent problems of CNTs. For example, the tubular structure of CNTs confines the electron emission to the apex region and thus shows a non-uniform emission for layered CNT films [12]. In addition, electrostatic shielding among the CNTs is negligible [13]. Therefore, the probe on developing other carbon cathodes is of both scientific and technical importance. As a promising alternative carbon material for fabricating cold cathodes, graphene has attracted more attention in recent years. Compared with CNTs, graphene has a high aspect ratio (lateral size to thickness), unique electrical properties, high transparency, intrinsic flexible structure and good mechanical properties [14,15]. Moreover, defective edge terminations of graphene was found to act as active emission sites to enhance the FE, which render graphene superior to CNTs for highly efficient electron tunneling with low voltage [16–21]. Great efforts have been made to make graphene layers vertically stand on substrates in order to fully take advantage of high field enhancement from atomic thin edges, such as vertically aligned few-layer graphene prepared by microwave plasma enhanced chemical vapor deposition method (CVD) [22,23], screen printing graphene films [16], and blade type electron emitter [21]. However, these means of vertically standing graphene (VSG) either involve fragile field emitter decays after voltage cycles or introduce contamination in graphene transfer process. So a simple method to prepare graphene lying flat on substrate with numerous, high field enhancement edge sites (FEES) is urgently needed.

Si is one of the most important electronic materials in view of device integration, which makes developing carbon cathodes on Si substrates being of particular importance. In the previous study, we reported the preparation and characterization of a novel Si hierarchical nanostructure, Si nanoporous pillar array (Si-NPA), and proved that Si-NPA was a micron/nanometer structural composite system with regularly pillar array surface morphology [24]. It was shown that field emission cathodes based on Si-NPA would largely reduce the electrostatic shielding among the emitters and might result in great increment of the field enhancement factor [13,25,26]. Herein we report a large-area graphene nanosheet (GNS) film was prepared by growing GNS directly

* Corresponding author.
E-mail address: lixj@zzu.edu.cn (X. Li).

https://doi.org/10.1016/j.mssp.2018.09.006
Received 2 May 2018; Received in revised form 26 July 2018; Accepted 3 September 2018

on Si-NPA substrate using Ni as catalyst via CVD method. The surface morphology and the microstructures of GNS/Si-NPA were characterized and the FE properties were measured and analyzed. Our results indicated that GNS/Si-NPA nanostructure might be a potential low-voltage cold cathode for practical applications.

2. Experimental details

Si-NPA substrates were prepared by hydrothermally etching (111)-oriented and boron-doped single crystal Si (*sc*-Si) wafers ($\rho = 0.015\,\Omega\,cm$) in a solution of hydrofluoric acid (13.00 mol/L) containing ferric nitrate (0.04 mol/L). The etching process was performed at 140 °C for 30 min (min) [24]. Thereafter, a layer of Ni nanocrystallites (*nc*-Ni) was deposited on Si-NPA substrate as catalyst for GNS growth by a chemical bath deposition method. The process of Ni deposition was as follows: a solution containing 0.2 mol/L nickelacetate and 4.0 mol/L ammonium fluoride was prepared in advance, adjust PH of the aqueous solution to 8 by aqua ammonia and then immerse the Si-NPA into the solution for 15 min. A layer of *nc*-Ni would precipitate on it gradually and the sample was named as Ni/Si-NPA. After that, the Ni/Si-NPA substrate was placed at the flat-temperature zone of aquartz tube for the subsequent GNS growth by CVD method. By keeping on protective gas mixture of high-purity hydrogen and argon (H_2:Ar = 65:200 standard cubic centimeter per minute (sccm)) blowing, the furnace was heated up to 1000 °C at a rate of 10 °C per min. Then methane gas was flowing into the protective gas at a rate of 10 sccm. After the growing process of graphene lasted for 5 min, shut down the methane gas and move the furnace out of the sample location. The sample was cooled down to room temperature (25 °C) quickly in ~10 min under the protective flow. The gotten product GNS/Si-NPA was named sample I. For comparison, GNS/Si-NPA with a longer CVD GNS growth time (10 min) was also prepared under the same preparing conditions and was named sample II.

The crystal structure and the graphitization degree of as-grown GNS/Si-NPA were characterized by an X-ray diffractometer (XRD, PA National, X′ Pert Pro) using Cu Kα1 radiation as the X-ray source ($\lambda = 0.15406$ nm) and a micro-Raman scattering spectrometer (Raman, RM-2000, Renishaw) with laser wavelength 531 nm. The surface morphology and microstructure of GNS/Si-NPA were characterized by a field emission scanning electron microscope (FESEM, JSM-6700F, JEOL) and a high resolution transmission electron microscope (HRTEM, JEM-2100, JEOL). The FE measurements were carried out by using a diode structure in a vacuum chamber at pressure of $\sim 2 \times 10^{-4}$ Pa at room temperature. An indium tin oxide (ITO) coated glass ($\rho = 8 \times 10^{-4}\,\Omega\,cm$) was used as the anode. The anode and cathode were separated by an insulating sheet of mica with a distance of 375 μm. The total emission area was 0.9 × 1 cm. The voltage applied was increased from 0 V up to 2500 V, with a step of 50 V. The current–voltage data were recorded with a digital multimeter (Sourcemeter-2400, Keithley) and then transferred to the current density-electric field (*J-E*) data correspondingly. The FE properties were analyzed according to the Fowler-Nordheim (F-N) theory combined with the morphological and structural features of as-prepared samples.

3. Results and discussion

Fig. 1(a) displayed the XRD pattern of the as-prepared sample I (bottom) and sample II (top). For sample I, three distinct diffraction peaks located at ~44.6°, ~52.0° and ~76.7° were observed obviously, and they were indexed to the (111), (200) and (220) family planes of cubic Ni (JCPDS No.04–0850), respectively. Based on the Scherrer's formula, the average grain size of *nc*-Ni zhaias calculated to be ~11.1 nm using the built-in X′Pert HighScore Plus software. For sample II, besides the three diffraction peaks for cubic Ni, another weak diffraction peak at 26.2° emerged, and it was assigned to the diffractions from the (002) reflection planes of graphene. In addition, the full width at half maximum (FWHM) of Ni peaks became narrower compared with those from sample I, which indicated the increment of the grain size and the improvement of the crystallinity of *nc*-Ni under 1000 °C CVD process for a longer time (10 min). According to the Scherrer's formula, the average grain size of *nc*-Ni increased to ~21.6 nm and that of graphene was calculated to be ~17.1 nm. No graphene diffraction peaks in sample I might be due to less graphene mass on Ni/Si-NPA, which could not be detected by XRD.

For further clarifying the bonding status of the carbon atoms in as-grown GNS/Si-NPA, the corresponding Raman spectra were measured and the results were presented in Fig. 1(b). Here two most intense peaks were observed in sample I and II, located at 1583.0 cm^{-1} and 2700.0 cm^{-1} separately, and they were indexed to the called *G*-band and *2D*-band correspondingly [27,28]. In addition, two peaks of *G** at 2452.0 cm^{-1} and *2D′* at 3248.0 cm^{-1} were present in sample I [29,30]. According to the previous studies on the Raman spectra of carbon materials, the *G* peak involved the band-stretching motion of the pairs of *C-sp²* atoms and *2D*-band was the second order of zone-boundary phonons [27,30]. *2D*' originated from phonons with opposite wavevectors of *2D* in order to satisfy momentum conservation, so it need no defects to active and was always present. *D* band, which was due to the breathing mode of six-atom carbon rings and need defects to active, was always used to label the defect degree of graphene [31]. Therefore, the presence of *G* band meant the sample contains *sp²* carbon networks, while the absence of the *D* band indicated the absence of defects in sample I and sample II. However, *G** peak, which assigned to a combination of *D* phonon and a phonon set at ~1100 cm^{-1} under visible excitation and always appeared in defected samples, was presented in sample I. It is reported that some defects such as perfect zigzag edges, charged impurities, intercalants, uniaxial and biaxial strain were non-

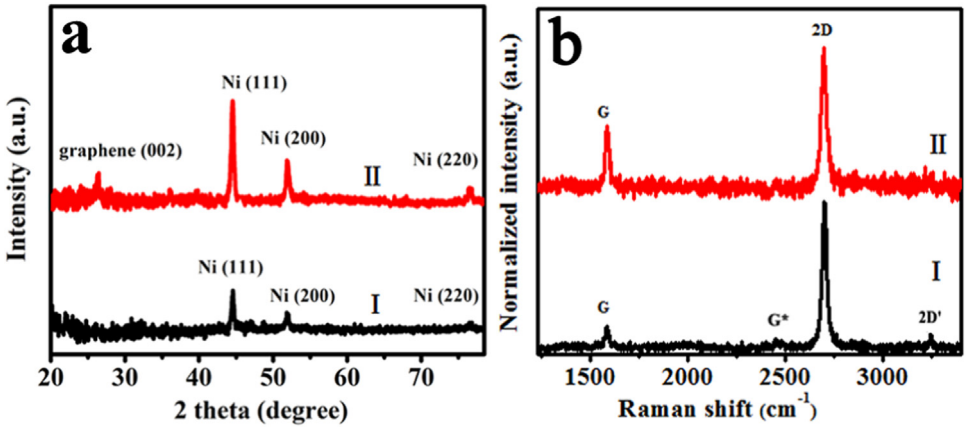

Fig. 1. (a) XRD patterns of GNSs with 5 min (sample I) and 10 min growth time (sample II). (b) Raman spectra of sample I and sample II.